Spring 5-1-2010

Evaluation of Quasi-Static Indentation Damage in Aluminum Honeycomb Core - Graphite/Epoxy Sandwich Structures

David Eisenberg

Evaluation of Quasi-Static Indentation Damage in Aluminum Honeycomb Core - Graphite/Epoxy Sandwich Structures

A Capstone Project Submitted in Partial Fulfillment of the Requirements of the Renée Crown University Honors Program at Syracuse University

David Eisenberg

Candidate for B.S. Degree
and Renée Crown University Honors

May/2010

Honors Capstone Project in Mechanical Engineering

Capstone Project Advisor: _____
Dr. Barry D. Davidson

Honors Reader: _____
Dr. Alan J. Levy

Honors Director: _____
Samuel Gorovitz

Date: _____

Abstract

Sandwich composites utilize a low density core and relatively stiff face sheets. These structures are ideal for applications that require high compressive strength, high bending stiffness, and very low weight such as aerospace vehicles. However, one problem with sandwich composites is their susceptibility to low velocity impact damage. Low velocity impacts result in both external damage, in the form of dents, and internal damage, in the form of core crushing, face sheet delaminations (two adjacent plies separating from one another), fiber fractures and matrix cracks. In general, it is assumed that visibly evident damage will be repaired. Barely visible impact damage (BVID) therefore represents a threshold, such that damage of this size or smaller must be considered to exist in flight structure, and structure must therefore be designed to tolerate this level of damage without a loss in performance. In order to design structures appropriately, it is necessary to understand the type and extent of internal damage present at or near the BVID threshold. Such damage assessments are then used as input for structural performance determinations.

The purpose of this paper is to investigate how structural and impact parameters affect the nature and extent of damage in sandwich composites in the vicinity of BVID. The particular sandwich composites that were studied are comprised of an aluminum honeycomb core and face sheets made from multiple plies of unidirectional graphite fibers in an epoxy matrix. The plies in the face sheets have fibers oriented in the 0°, 90°, 45° and -45° directions. These plies are relatively stiff in the fiber direction and compliant in the perpendicular direction. Plies of different directions are stacked on top of each other to build face sheets that are quasi-isotropic, i.e., that have the same strength and stiffness in their in-plane directions. The parameters that are investigated in this paper are the core thickness, core density, face sheet stacking sequence (the sequence that the plies in various directions are placed on top of one another), load, and indenter diameter. To this end, specimens are indented using a quasi-static indentation test. In this test, load is applied monotonically using a fixed diameter indenter until the permanent dent becomes barely visible. This approach has been shown to produce essentially the same type of damage as low-velocity impact, but allows for more consistent and controllable levels of damage to be created. The damage was then evaluated non-destructively via ultrasonics and destructively via cross sectioning and microscopy. The results obtained by these two methods were then compared and synthesized to obtain an understanding of the internal state of damage as a function of those parameters studied. It was found that the two parameters that are most important are the face sheet stacking sequence and the core density. In terms of stacking sequence, delaminations are most prominent between plies with large differences in their fiber orientations. For adjacent plies with very different fiber directions (i.e., a 90° ply followed by a 0° ply), there is a large mismatch in stiffness and in coefficient of thermal expansion. This causes large shear stresses, which in turn lead to delamination. In addition, stiffer, higher density cores are observed to cause more delamination to occur than lower density, more compliant cores. It is expected that the data and trends collected in this study may be used to provide guidance for choosing structural geometries that optimize weight, cost, and impact resistance for practical structural applications.

Table of Contents

- Acknowledgements p. 4
- Research Essay pp 5-43
  - Introduction pp. 5-9
  - Background Information pp. 9-12
    - Types of Damage pp. 9-11
    - Previous Work pp. 11-12
  - Materials and Methods pp. 12-24
    - Composites and Nomenclature pp. 12-14
    - Panel Manufacturing pp. 14-15
    - Quasi-Static Indentation Test pp. 15-17
    - Indentation Profile Evaluation pp. 17-18
    - Internal Damage Evaluation pp18-24
  - Results pp24-41
    - Non-Destructive Evaluation pp. 24-27
    - Destructive Evaluation pp. 27-31
    - Effect of Specimen Size pp. 31-35
    - Damage Resistance pp. 35-41
  - Conclusion pp. 41-43
- Sources Cited and Consulted pp. 44
- Appendices
  - Appendix A
  - Appendix B

Acknowledgments

I'd like to thank my research advisor, Dr. Davidson for getting me into this project, overseeing everything and helping me along the way. I'd also like to thank Abhen Singh for working on the project with me and Dr. Levy for being the honors reader and always being there to advise me on whatever I need.

This work was co-supported by the NASA Constellation University Institutes Project, Grant NCC3-989, Claudia Meyer, Project Manager and by the Exploration Technology Development Program/Advanced Composites Technologies Project, Mark Shuart, Project Manager

I. Introduction

The options for materials that engineers have available to them have become more varied over the last century, particularly in terms of composite materials. Composite Materials refer to any material that is composed of multiple, different materials combined on a macroscopic scale. This is different than a material such as an alloy. An alloy is a solution of multiple metals. Here the metals are combined on a microscopic scale and the atoms are distributed as such. Conversely, reinforced concrete is a typical composite, where the reinforcing steel rods are easily distinguishable from the concrete "matrix." Unfortunately, as the materials themselves become more complex, it becomes increasingly difficult to understand how they will function in various situations. It is crucial that the mechanisms by which composites fail and the factors that influence it are more thoroughly understood.

Composites are extremely advantageous in a variety of ways. Firstly, because they can take advantage of a far wider array of materials than traditional engineering materials, they are capable of having a far greater strength to weight ratio than metals or ceramics. Most engineering metals respond in the same way regardless of the direction of the stress. Materials that exhibit this behavior are called isotropic. Composite materials can be more precisely designed so that they have a lot of strength in specific critical directions while not wasting size and weight to maintain strength in non-critical directions. Materials that act differently depending on direction are known as anisotropic.

Composite materials have a wide array of possible applications; one important application is in NASA's new Ares I rocket. NASA is funding this project because in a device such as a rocket, the strength to weight ratio is extremely important. By being able to use composites with a greater strength to weight ratio than traditional materials NASA can save significant amounts of money on energy costs.

One widely used class of composites is laminated composites. Laminated composites are comprised of multiple plies or layers. One type of laminated composites which is of particular interest is those that use continuous carbon fiber reinforcement. In plies of this type of material, carbon fibers are oriented in a particular direction and held together in an epoxy matrix. Multiple plies of these carbon fiber matrices can be stacked on top of one another creating a composite laminate. Each ply exhibits exceptional strength in the fiber direction but is relatively susceptible to failure in the non-fiber direction. As will be described subsequently, the laminate is also susceptible to failures that occur in-between the individual plies.

The strength of a material can be thought of as its resistance to a particular type of force. In order to produce a material that can handle forces in different directions, plies can be stacked on top of one another, each with fibers in one of several directions. When the plies are stacked in such a way that there are fibers pointing in the 0°, 90°, 45°, and -45° directions and the fiber direction of each ply is symmetric about the midplane of the stack, then the laminate is said to be "quasi-isotropic." This means that it will respond the same way to a force that is

applied in any in-plane direction. It will respond differently to a force in the out-of-plane, or through the thickness direction, and for this reason it is only quasi-isotropic and not isotropic.

Laminated composites for space vehicle applications are typically designed for compression and bending loads. A material's resistance to bending stresses is highly dependant on its second moment of area, which is a function of its thickness. By increasing the structure's thickness, one can improve its resistance to bending stresses. The obvious method of increasing the structure's thickness is to add additional plies. However, while increasing thickness and resistance to bending stresses, this also increases weight. Since one of the main benefits of the carbon fiber composite is its low weight, added weight somewhat defeats the purpose of the laminate in the first place. On the other hand, if a low-density material were placed in the middle of the laminate, then this would increases the thickness of the structure, and hence its resistance to bending, without a significant weight increase. This type of approach is referred to as a "sandwich structure" and is illustrated in Fig. 1. The low density material is the core and the high stiffness and strength material comprise the face sheets. Sandwich structure can have metal face sheets. When the face sheets are comprised of a laminated composite, this type of arrangement is typically referred to as a sandwich composite. Sandwich composites therefore provide a

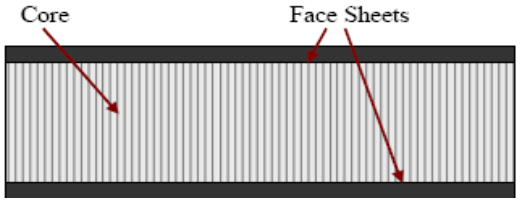

Figure 1. Sandwich Composite
Diagram of typical sandwich composite with face sheets on both ends and the core in the middle

highly effective approach to improving a laminate's resistance to bending. Here the face sheets bare the majority of the load while the core is designed primarily to increase the material's thickness. This effect is similar to that of an I-beam.

Although these sandwich composites possess low weight along with the desired properties of good resistance to bending and compression, they are also susceptible to low velocity impact damage. A low velocity impact could occur in various stages of the material's lifecycle. For instance, during assembly, tools could be dropped upon the specimen or during use, debris or other materials could bump into the panel causing a low velocity impact.

Low velocity impacts result in both external damage, in the form of dents, and internal damage. Internal damage can take various forms such as core crushing, which refers to buckling within the cell walls of the core. Another common damage type is face sheet delaminations, which are two adjacent plies separating from one another. Fiber fractures may also occur, which are breaks in the carbon fibers. Finally, matrix cracks may also result from low velocity impact. These are cracks within a single ply that propagate within the epoxy and parallel to the fibers. In general, it is assumed that visibly evident damage, such as panels with large dents will be repaired but damage that is invisible or only barely visible to the naked eye could go unnoticed. Barely visible impact damage (BVID) therefore represents a threshold, such that damage of this size or smaller must be considered to exist in flight structure, and flight vehicle structures must therefore be designed to tolerate this level of damage without a loss in performance. When dealing with metals, one can generally say that if an impact causes little or no

external damage, then there is little or no total damage. This cannot be said about sandwich composites. Even if there is little or no visible external damage, there can be enough internal damage to render the panel structurally unsound.

This study investigates the damage induced in sandwich composite specimens if they undergo a low velocity impact, and how various parameters affect that damage. The parameters investigated in this study are the core thickness, core density, face sheet stacking sequence (the sequence that the plies in various directions are placed on top of one another), load, and indentor diameter. A parallel and complementary study is being performed that investigates how much planar compressive strength is lost due to BVID. The results from my study are directly used in this complementary study, as it allows the correlation of various specific damage types to the observed strength loss. Thus, the results of this research are two-fold. First, my study will directly provide knowledge of how different structural and impact parameters affect the internal damage in a sandwich composite. The parallel strength study will provide knowledge about how each type of damage affects the structure's strength. This information may then be used by NASA to choose appropriate structural configurations that will be the most impact resistant.

II. Background Information

A. Types of Damage

As stated earlier, low velocity impacts often result in dents that are difficult to see but indicate significant internal damage. As previously described, this internal

damage manifests in a variety of ways. Core crushing, i.e., when the cell walls of the core buckle will accompany any sizeable dent. A photograph illustrating core buckling is presented in Fig. 2. Another type of damage that can occur is face sheet debonding, which occurs when the face separates from the core. One type of damage that the face sheet may undergo is known as delamination. Delamination is when two adjacent plies separate from one another. Another type of damage that can occur is a matrix crack. Matrix cracks are cracks that go across a ply in the face sheet instead of just at the interface of two plies such as a delamination. a photomicrograph displaying interface delaminations and matrix cracks are is displayed in Fig. 3. The last type of damage that can occur is fiber failure, which is when the individual fibers in the face sheet break.

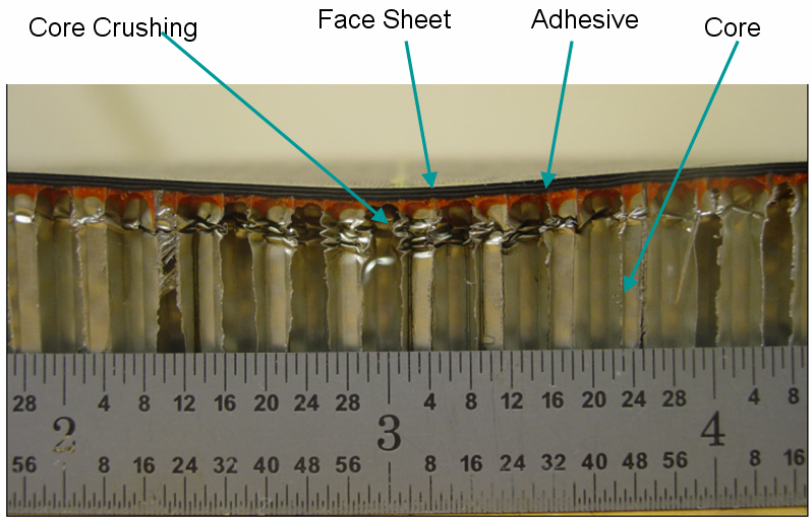

Figure 2. Cross Section of damaged panel
The buckling of the cell walls within the core is clearly visible in this specimen cross section

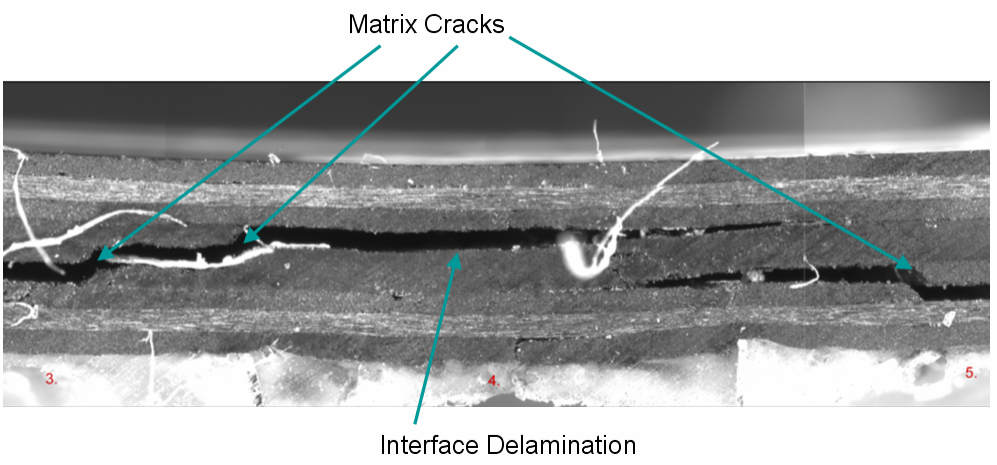

Figure 3. Magnified image of damaged face sheet
In this magnified image of a damaged face sheet, the interface delaminations and matrix cracks are clearly visible.

B. Previous Work

Other studies have been performed on impact resistance of composite structures and even impact resistance of sandwich composite structures. Previous experiments have suggested that one major damage mode in thin composite panels subjected to a low velocity impact is interface delamination.[1] This suggests that measuring the total amount of delamination that occurs within the face sheet is essential to understanding the damage state.

Previous experiments have also determined that the size of the delamination at the interface between two plies is dependant upon the mismatch of thermal and mechanical properties of adjacent plies.[2] During the cure cycle of manufacturing, the plies are heated and expand, if adjacent plies expand at different rates or in different directions, then there are residual stresses left in the plies after they cool. Also, different Young's modulus and shear modulus (properties that characterize the way a material reacts to normal stress and tangential stress respectively) of

adjacent plies contributes to how the specimens delaminate. The plies are very stiff in the fiber direction and pliant perpendicular to the fiber direction, so the difference in thermal and mechanical properties from one ply to an adjacent ply referenced previously is due to the different orientation of one ply to an adjacent ply. This suggests that the stacking sequence of the face sheet is extremely important.

III. Materials and Methods

A. Composites and Nomenclature

The sandwich composites used in this study are composed of an aluminum honeycomb core and face sheets made from multiple plies of unidirectional carbon fibers in an epoxy matrix. The fibers are IM7 carbon fibers which exhibit an intermediate modulus and intermediate strength. The epoxy is 8552 epoxy which is a toughened epoxy designed for high strength, stiffness, and damage resistance. The core is 5052 aluminum honeycomb shaped with cells that are 3.175mm long. A diagram of the core is presented in Fig. 4. Due to the shape of the cells, there is directionality to the core. For this study, during manufacturing, the ribbon direction as shown in Fig. 4 was always aligned with the 0° ply. Three different versions of this core are used. See table 1. The differences between the different versions are based on the thickness and density of the core.

Table 1. Core Types

Designation	Thickness (mm)	Density (kg/m^3)
C1	25.4	49.7
C2	16.5	49.7
C3	25.4	72.1

Table 2. Layup Types

Designation	Sequence
Q1	$[45/0/-45/90]_s$
Q2	$[45/-45/0/90]_s$
Q3	$[-45/45/90/0]_s$

The plies in the face sheet are stacked on top of one another in various orientations with each ply in the 0°, 90°, -45°, or 45° directions. Each face sheet is made from eight plies stacked on top of one another in a particular orientation. Table 2 lists the three face sheet layups used in this study. The convention is to list the first four plies; the last four are a mirror image of the first four so that the face sheet is symmetric about the mid plane. This allows the face sheets to be quasi-isotropic. The core is bonded to the face sheets by 3M AF-555 adhesive which is designed for honeycomb bonds. Figure 5 presents an exploded view of the sandwich composite.

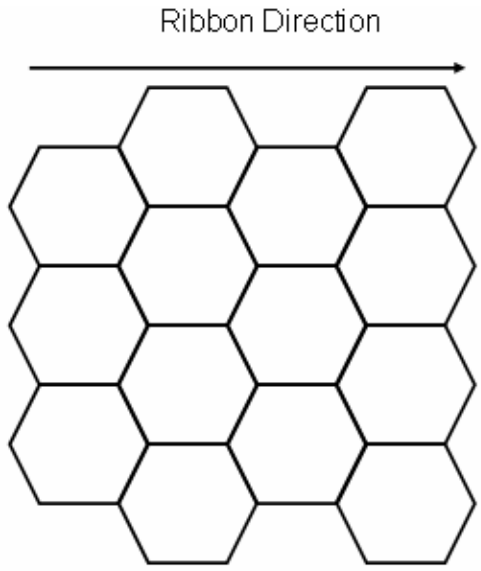

Figure 4. Diagram of Honeycomb Core
The shape of the cells of the core is shown along with the ribbon direction.

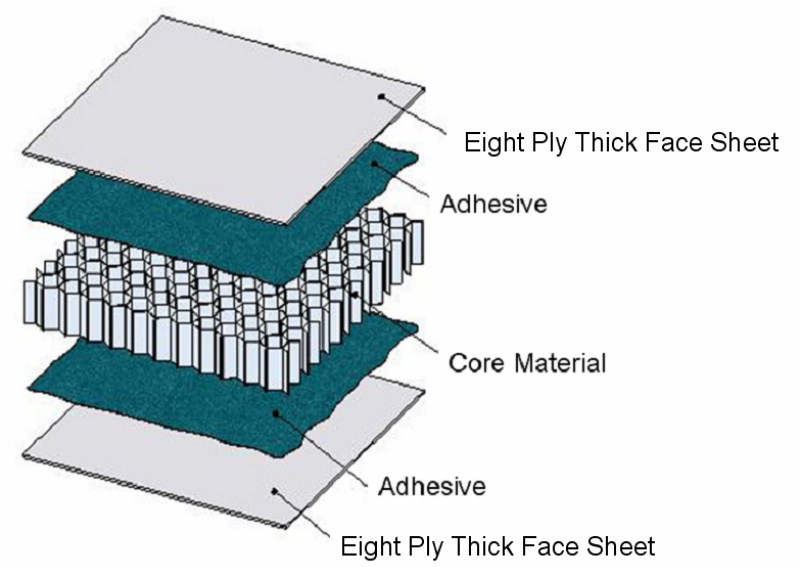

Figure 5. Exploded View of Sandwich Composite[7]
Each layer is shown in relation to every other layer.

B. Panel Manufacturing

All of the specimens used in this study were manufactured in-house. To this end, the individual plies in the face sheet are first cut from a long roll of IM7/8552 graphite epoxy. The plies are then stacked on top of one another according to the face sheet lay up for that particular panel type. Special care must be taken to keep all foreign particles off of the plies and to remove all of the air bubbles between plies. After both face sheets are made and labeled, they are stored at low temperature.

Once the face sheets are laid-up, the sandwich panel assembly process is initiated. First the top and bottom plates that will house the sandwich panel are sprayed with lubricant so that the face sheets do not bond to them during the cure cycle. Then the bottom face sheet is placed on top of the bottom plate and the adhesive is placed on top of the face sheet. The core is placed on the adhesive

with the ribbon direction aligned with the 0° direction and another layer of adhesive is placed on the core. Finally, the top face sheet is placed on top of the adhesive and the top plate on top of the face sheet. Then the whole assembly is wrapped in breather cloth to provide padding and to aid in the removal of air during the cure process.

Next, the assembly is wrapped in vacuum bagging material with a vacuum hose attached and a vacuum is pulled. It is then placed in an autoclave to cure. During the cure cycle, the autoclave applies heat and pressure to the sandwich panel. The pressure must be strong enough to remove any air bubbles from the face sheets and to provide a strong bond, but not so strong that it crushes the core.

The as-manufactured panels are 355.6 mm square. Test specimens were then cut from these panels. Some of these test specimens were cut as full size specimens (177.8 mm x 152.4 mm) which were designed for non-destructive evaluation only (as will be discussed later) and would also be used in the complementary residual compression strength study. The others were cut as small specimens which could then be destructively evaluated (as will be discussed later). Since the costs associated with manufacturing the sandwich composites are significant, it is desirable to have the specimens that are destructively evaluated to be as small as possible without affecting the results. Small specimens that were to be indented under the 25.4 mm diameter indentor were cut to be 75 mm square and those that were to be indented under the 12.7 mm diameter indentor were cut to be 50 mm square.

C. Quasi-Static Indentation Test

The Quasi-Static Indentation (QSI) test is used to simulate the low velocity impacts that are the focus of this study. In this test, load is applied monotonically to a fixed diameter, spherical indentor until the specimen fails or a dent becomes barely visible. The indentor moves with a constant velocity of 0.00508mm per second and can have a diameter 12.7mm or 25.4mm depending on the test. The tests are stopped when a dent becomes barely visible because as stated earlier, (see Section I) barely visible impact damage is the focus of this study. Figure 6 presents a photograph of the QSI setup.

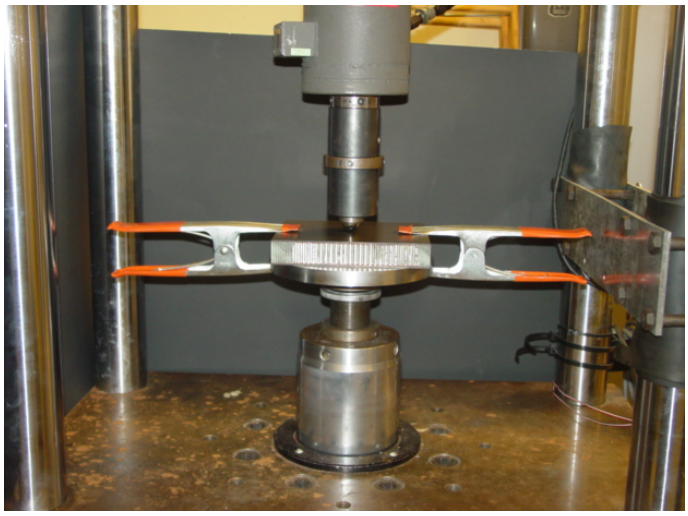

Figure 6. QSI Setup
The Indentor is seen just above a specimen

Hypothetically, a low velocity impact would not occur in a quasi-static manner; instead, it would happen dynamically. However, according to various studies, the damage type and damage extent caused by quasi-static tests and dynamic tests are virtually identical.[3-6] This means that the QSI test should adequately mimic the damage that can occur within a specimen due to impacts caused by debris or other foreign objects.

The QSI tests are designed to produce BVID in specimens with a 12.7mm or 25.4mm diameter indentor. In order to be able to compare specimens, it is important to indent specimens under a consistent load or to a consistent indentation depth. A dynamic test can have a set load and drop height, but it is impossible to set an indentation depth. This is where the quasi-static test has an advantage over a dynamic test. It allows the user to not only indent to a given load, but it can also indent to a given depth. Since the QSI test accurately mimics the damage induced via dynamic impact (as stated earlier) and provides additional control, the QSI test is the ideal method for impacting the specimens to be studied.

D. Indentation Profile Evaluation

In this study, it is essential to measure the size and depth of the permanent dent left in the specimens. This must be done because there needs to be a metric in order to determine whether a dent is invisible, barely visible, or clearly visible. Also, the dent itself is an important type of damage which can affect the residual strength of the material.

The permanent dent left in the panels due to the QSI test was evaluated using ultrasonic inspection. The Syracuse University Composite Materials Laboratory c-scan unit, which employs a 500MHz transient waveform digitizer, was used to accomplish this task. The c-scan unit is essentially a tank filled with water that uses a transducer to send waves at a specimen. The c-scan then measures the time of flight of the waves and by knowing the speed of the waves in water, one can reconstruct the surface profile.

The surface profiles were verified by checking the c-scan results against a mechanical surface profile measurement system. This system consists of a dial gauge mounted above a precision sliding x-y scale. The c-scan approach was found to be both accurate and efficient. Figure 7 presents an example of a typical surface profile measured using the c-scan. Here, the flat surface is the top surface of the specimen. From this type of surface profile, the depth and size of the dent can easily be ascertained.

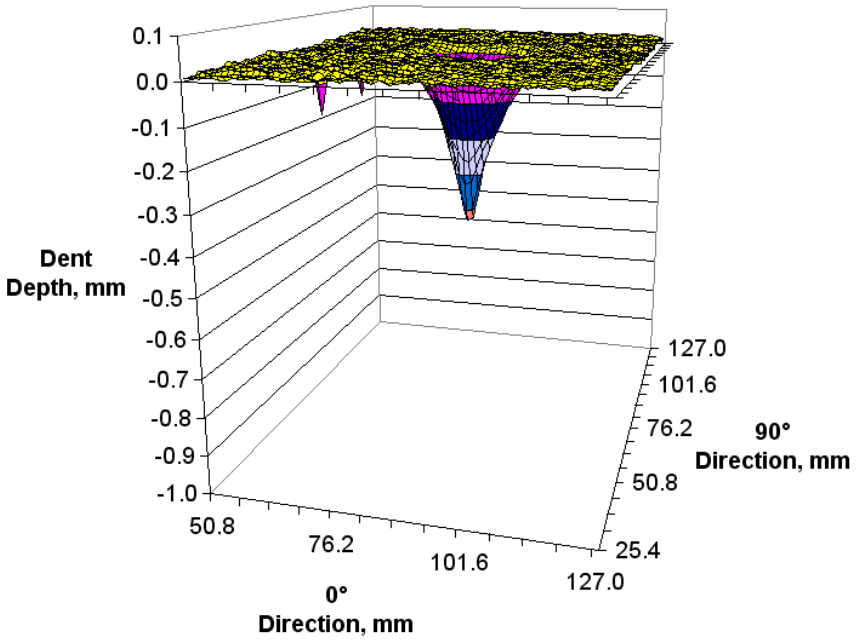

Figure 7. Dent Profile
Typical dent profiles using 25.4mm diameter indentor obtained via c-scan.

E. Internal Damage Evaluation

The c-scan was also used to evaluate the internal delaminations. The internal delaminations are a major damage source and a possible determinant of residual compressive strength. Instead of having the c-scan record reflections from the top

surface of the specimen, it can be set to record reflections from delaminations within the specimen. Since a delamination occurs at a set interface, one can accurately tell where a given delamination is within the face sheet based on the time of flight data. In this way, a top down view of the delaminations within the specimen can be mapped without having to cut the specimen apart in any way. A sample delamination evaluation from the c-scan is shown in Fig. 8. In this image, the time of flight is displayed by the color. Longer times of flight are closer to red along the color axis shown on the right. The colors representing delaminations at different interfaces are displayed along the axis to the right. In this image, one can clearly make out delaminations in three distinct interfaces shown in blue, green, and yellow (interfaces 3, 5, and 6.)

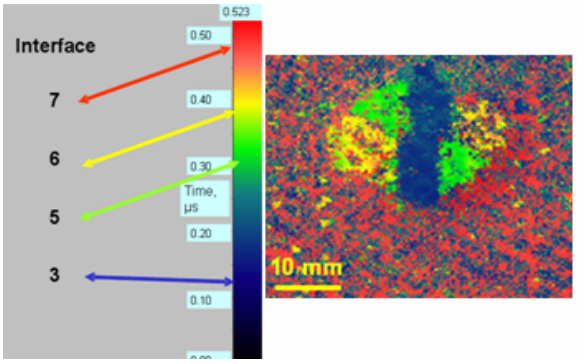

Figure 8. Typical c-scan Image
A typical image of face sheet delaminations obtained via c-scan.

Since this method leaves the specimen intact, it is referred to as non-destructive evaluation. The non-destructive approach has some key features that make it advantageous. Firstly, it leaves the specimen intact so that it could continue use. Secondly, the c-scan works rather quickly. Finally, it provides a "global" picture when compared to other methods. By global, I mean that it gives

the user a sense of general trends such as the relative shape, position, and orientation of delaminations.

However, the non-destructive evaluation also has some drawbacks. The c-scan works from the top down, so delaminations in lower interfaces can be hidden, or "shielded," by delamination in upper interfaces. Also, the resolution of the c-scan is not fine enough to pinpoint damage types such as matrix cracks of fiber failures.

All specimens (both large and small) were evaluated non-destructively. In order to be able to validate the conclusions drawn from the c-scan images and in order to fill in the gaps from the c-scan image such as delamination in the shielded regions, the small specimens were destructively evaluated. We did this working under the assumption that the data gathered from the destructively evaluated small specimens should be applicable to the large specimens as well. In order to destructively evaluate the specimens, they were cross-sectioned. The cuts were made through the dent center using a thin diamond blade.

After cutting, specimens were imaged using a "scanning optical microscope," i.e., a microscope that takes several images across a large planar area, auto-focuses at each, and then reconstructs the grid of images to correspond to the actual specimen. These images are then inspected so that the delaminations and matrix cracks can be identified and quantified.

From the photomicrograph, "2D damage maps" were constructed. These are scale drawings that elucidate all of the pertinent information such as delaminations and matrix cracks. They were designed for our own ease-of-use so

that we would not need to continually refer back to the photomicrographs. Figure 9 presents a typical photomicrograph and its corresponding 2D damage map.

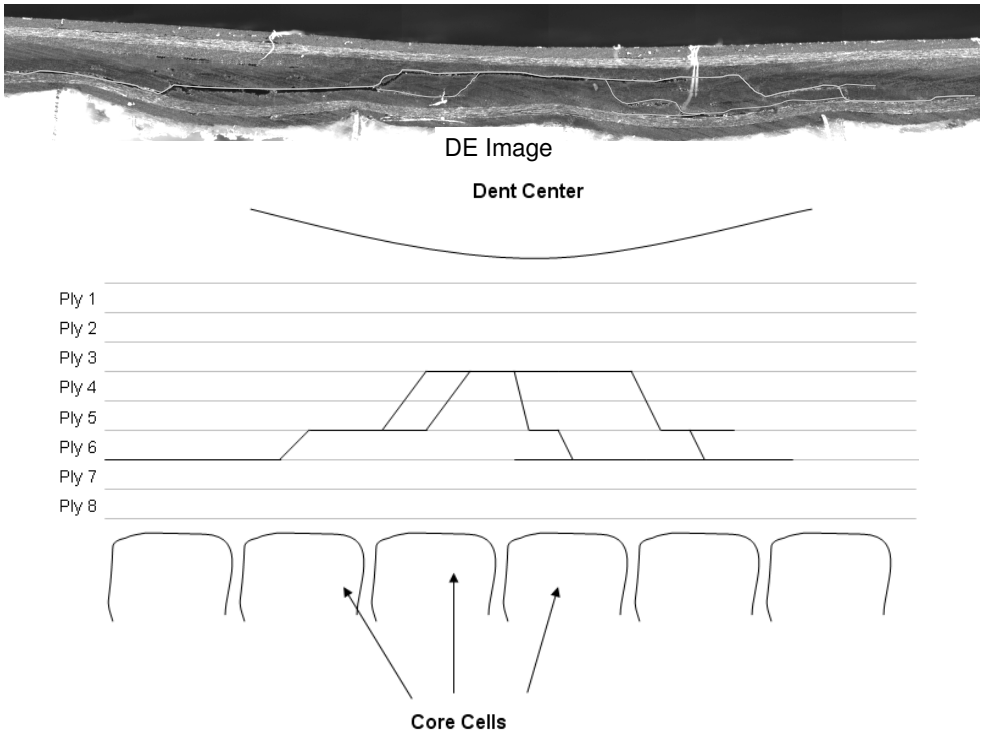

Figure 9. Photomicrograph and 2D Damage Map
Above is photomicrograph with the delaminations highlighted so that they are easier to see and below is the corresponding 2D damage map

It was observed rather early in the study from the c-scan images that the delaminations are generally oblong and that the major axis of the delaminations tends to follow the fiber direction of the back surface ply. That is, if there is an interface delamination between a 90° ply on top of a 45° ply, the major axis of the delamination will be along the 45° direction. Due to this pattern, a relatively comprehensive understanding of the damage state can be constructed from cross sections in the four principle directions (0°, 90°, -45°, and 45°.) So, the cross sections were only performed in these four principle directions. Four 2D damage maps were then constructed from the photomicrographs obtained from the cross

sections. These four 2D damage maps were then synthesized into a “3D damage map.” Figure 10 presents a typical 3D damage map. The 3D damage map consists of multiple XY graphs (one for each interface). The origin of the graph is located at the center of the dent and delaminations as seen from the photomicrographs are represented by solid colored lines. Since the majority of damage only occurs in certain interfaces, only those interfaces are displayed when showing a 3D damage map.

The 2D damage maps are side views, and the c-scan images are top down views, this means that they cannot be directly compared. The 3D damage maps however, are top down views, so, the c-scan images can be directly compared to the 3D damage maps. In this way, we can determine how well non-destructive and destructive evaluations correlate to one another.

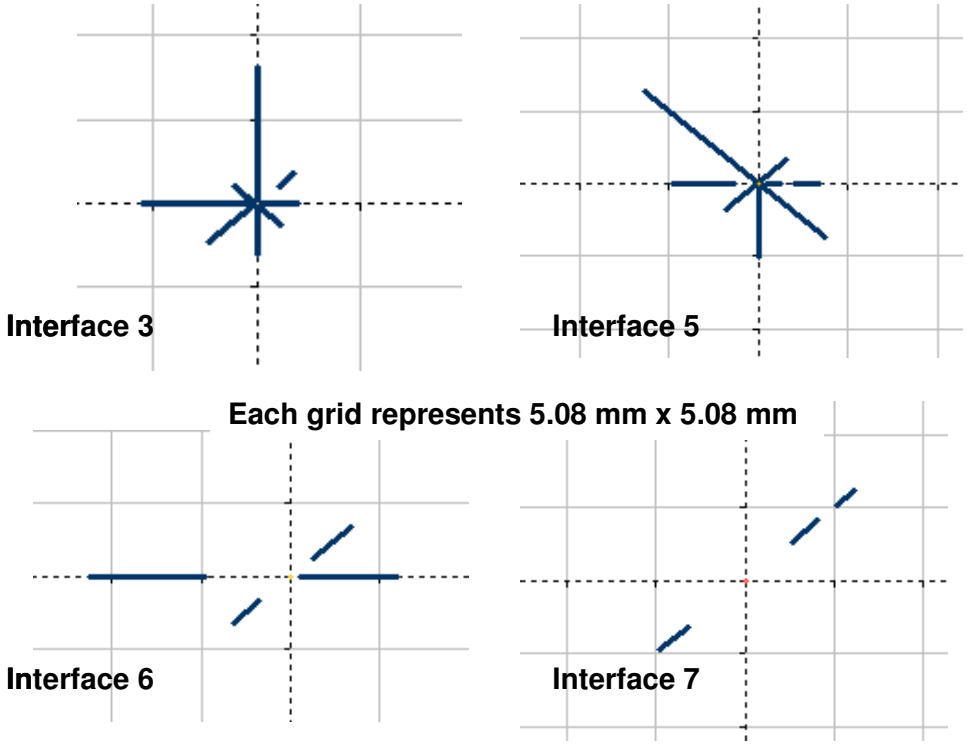

Figure 10. 3D Damage Map
A typical 3D damage map. The solid lines represent delaminations seen from the cross sections of this specimen.

The destructive evaluation has some important advantages over the non destructive methods. Firstly, since the images are from cross sections, they are side views and there are no issues with shielding (i.e. delaminations in upper interfaces do not hide those in the lower interfaces.) Also, since the images are side views, one can clearly discern matrix cracks and core crushing, which cannot be done with the non destructive images.

There are also significant problems with the destructive evaluation. Once the specimen has been cross sectioned, it is generally useless for any other purpose and a compression after impact test cannot be performed on it. Also, since multiple cross sections and optical scans are needed, the destructive method is tedious and time consuming. Finally, the destructive method only gives four

snapshots of the damage state that must be synthesized in order to understand the holistic nature of the internal damage. It is difficult to discern the general damage state that exists within the specimen without a c-scan image to supplement it.

IV. Results

The purpose of this study is to evaluate the BVID induced in sandwich specimens subjected to low velocity impacts (modeled as Quasi-Static Indentation). Toward this end, all of the specimens are evaluated non-destructively via the c-scan machine. Then, in order to verify conclusions drawn from the c-scan images as well as gather data on areas that the c-scan images cannot see (such as shielded regions), the small specimens are destructively evaluated via cross sectioning. From these results, for each panel type, it is determined where the different types of damage occur and their extents. As part of this, it is important to evaluate whether there are any size effects over the range of sizes chosen. That is, does the damage induced within the small specimens match that damage induced within the large specimens? Finally, the results are to be synthesized in an effort to establish how each parameter studied affects the material's resistance to the various forms of BVID.

A. Non-Destructive Evaluations

Figure 11 presents typical c-scans of the three different face sheet layups from specimens that were indented with the 25.4 mm diameter indentor. The color scale and ply angle convention used here is the same as that introduced in Figure 8. Delaminations were observed only at interfaces 3, 5, 6 and 7. Also, delaminations at interface 7, depicted in red, are often difficult to distinguish from

the back surface reflection that is obtained in the regions where no delaminations exist. Note that for layup Q1, good information was obtained for interfaces 3, 5 and 6, with limited information at interface 7 due to shielding effect, i.e., the fact that the ultrasound cannot pass through a delamination to locate other delaminations that may exist beneath it. For Q2, the results are a bit worse due to the shielding of near-surface delaminations, and the scans for Q3 indicated only those delaminations at interfaces 3 and 5.

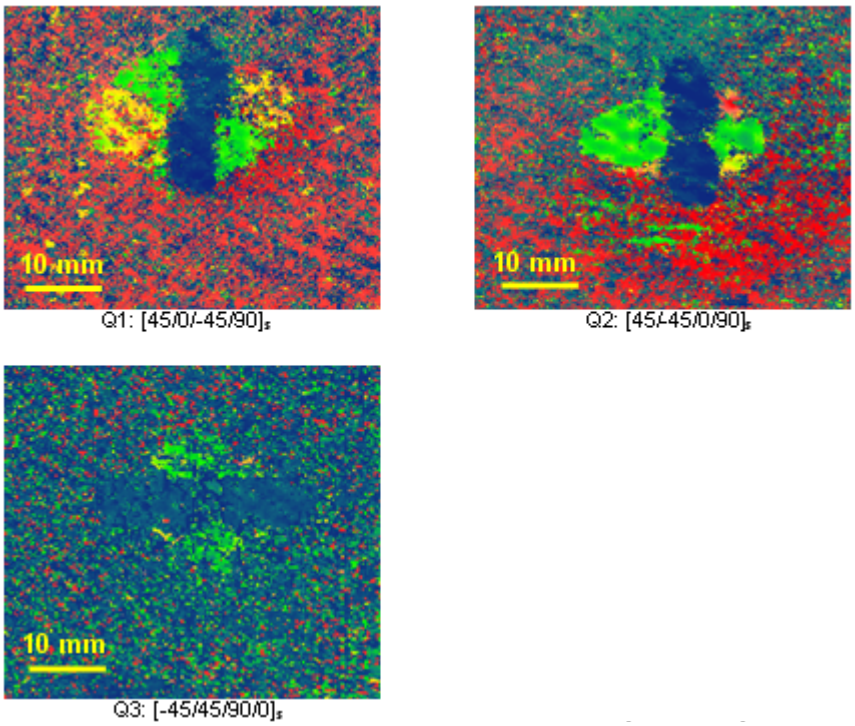

Figure 11. C-Scan Images
Typical c-scans for the four face sheet layups are shown.

For all panel geometries, if it is assumed that all delaminations are continuous through the shielded region, then all delaminations are oblong, with the direction of the major axis of each delamination primarily controlled by the direction of its back surface ply. This is similar to what has been observed in low velocity

impacts of non-sandwich laminates.[8] The delaminations at interface 3 were always lemniscates (peanut shaped). For layups Q2 and Q3, their major axis is aligned with their back surface ply angle, whereas for Q1, the two portions of the lemniscates are slightly offset, giving the major axis a slight tilt towards the positive 45° direction. Each layup has one other delamination at 0 or 90 degrees, which occurs at either interface 5 or 6, depending on the layup. These are either elliptical or lemniscate shaped. As in the case of interface 3, the interface 5 and 6 delaminations are aligned with the back surface ply angle for Q2 and Q3, but have a slight tilt towards the positive 45° direction for Q1. For all panel types, these are the widest delaminations of all that occur; for layups Q1 and Q2, they are also the longest.

Layup Q1 has tilted, lemniscate shaped delaminations at interface 3 and a somewhat longer and wider trapezoidal shaped delamination at interface 5. The largest delaminations occur at interface 6 in these face sheet types and are either elliptical or lemniscate shaped and are slightly tilted with respect to the back surface ply angle. The delaminations at interface 7 appeared to be smaller than those at interface 5. For Q2, the delamination at interface 3 was similar in shape to Q1, but somewhat wider, without any obvious tilt of the major axis. The largest delamination was oriented at 0° at interface 5 and was similar in size to the delaminations at interface 6 in Q1. The 45° delamination at interface 6 was smaller than the 45° delamination at interface 5 in Q1. The delamination at interface 7 was similar to Q1 in terms of size and. We had limited results for Q3, but the NDE data suggest that it had the longest and widest delamination at

interface 3 out of all layups. The delamination at interface 5 was wider but similar in length or perhaps a bit shorter than that at interface 3. The delaminations at interfaces 6 and 7 were similar to those seen in Q2 face sheet type.

As will be shown subsequently, the size of delamination distribution also differs between different core types. For the same face sheet, the delaminations are larger in panels with the C2 and C3 cores than in those with C1. The 0 and 90 degree delaminations are thinner and longer in C2 core type than in C1 and C3, where in the latter two they are similar sized.

B. Destructive Evaluations

The c-scan data was able to tell us where delaminations occurred as well as the relative size, shape, and orientation of those delaminations. Destructive evaluation is needed to corroborate those results within the small specimens as well as fill in information about the shielded regions in interfaces 5, 6, and 7. One important result obtained from the photomicrographs and their corresponding 2D damage maps is that the delaminations tend to only occur in interfaces 3, 5, 6, and 7. See Fig. 12 for a comparison between a c-scan image and a photomicrograph. There were an extensive number of photomicrographs taken and corresponding 2D damage maps created. In order to document these, Appendix A presents a brief description of each along with its file name and corresponding 2D damage map. The photomicrographs are contained within very large files and the individual features would be difficult to distinguish at the scale at which they would need to be presented in the appendix, so, a DVD with all of the photomicrographs corresponding to the files listed in Appendix A is included with this paper. On

occasion, there are small delaminations in interfaces 1 or 2 but they are usually significantly smaller than those in the four primary interfaces. This corroborates the results from the c-scan. Furthermore, there are never any delaminations in interface 4, which is the mid plane of the face sheet. For these reasons and the sake of brevity, when a 3D damage map is presented, only interfaces 3, 5, 6, and 7 are shown.

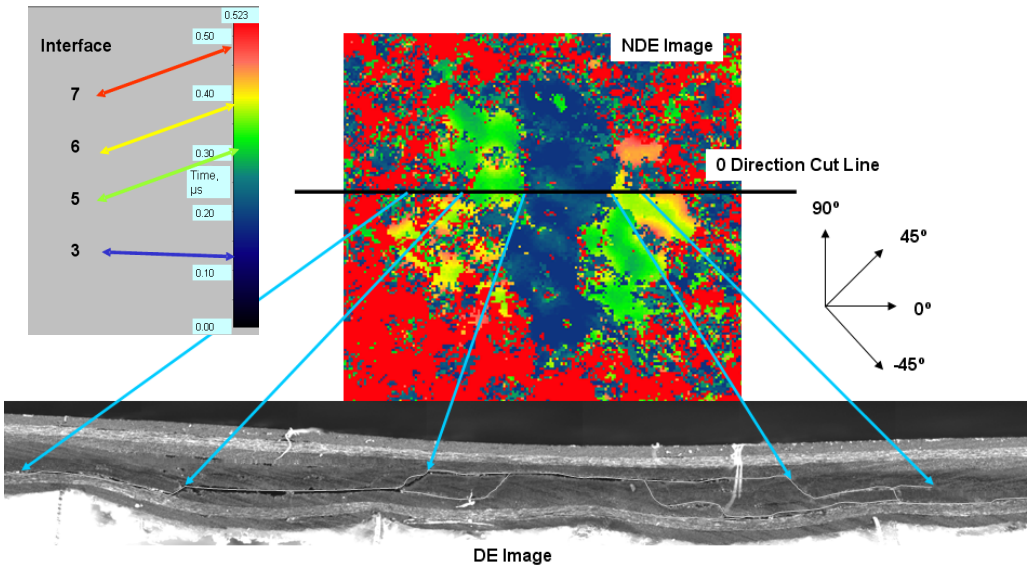

Figure 12. Comparison of c-scan image to photomicrograph.
The c-scan image is at the top with a scale along side it. The photomicrograph is below it with the delaminations enhanced for easier viewing. These images are taken from the same Q1-C1 specimen that is used for figure 5.

Appendix B presents the complete set of 3D damage maps developed as part of the study. As a typical example, Fig. 13 presents 3D damage map from Fig. 10 with NDE the data superposed on top of it. In this 3D damage map, the solid lines present the delamination information obtained at each interface from the section cuts. The light blue shaded regions represent overlays of the delamination information obtained by the NDE image for that particular interface. The light blue shaded regions are much smaller and are discontinuous through the dent

center in all of the lower interfaces because potential delamination in the center is shielded by delaminations in interface 3. With this in mind, it may be observed that these comparisons and those of Fig. 12 provide strong corroboration of the NDE results, and this was true in all specimens evaluated.

The dotted lines in Fig. 13 utilize the combination of the DE and NDE results to make a conservative estimation of the delaminated area at each interface. This was done primarily to better understand the nature of the shielded damage. By making these damage maps for multiple specimens of each configuration, it was possible to extract some general trends.

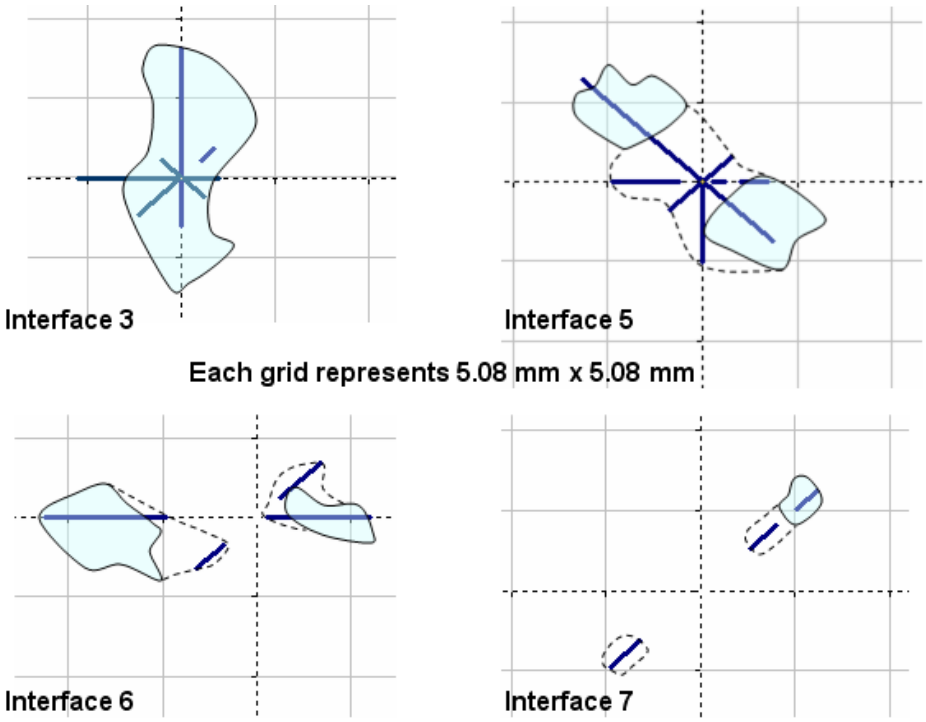

Figure 13. Enhanced 3D Damage Map
This 3D damage map includes the area of delamination obtained from the c-scan (light blue shaded regions) as well as an approximation at the shape of the delamination (dotted lines).

In Fig. 13, one can see that the delaminations in interfaces 3 and 5 are continuous through the dent center. However, the delaminations in interfaces 6 and 7 exist on either side of the dent center but seem to disappear in the middle. This indicates that just because one sees a delamination on either side in a c-scan image does not mean that the delamination exists through the middle. So, it is essential to analyze whether the delaminations are continuous through the shielded region or not in order to fill in the gaps in the c-scan data.

From these 3D damage maps, we see that for the Q1 layup, the delaminations at interface 7 are often discontinuous throughout the shielded region. For the Q2 and Q3 layups the delaminations in interface 6 are not always continuous through the shielded region and the delaminations at interface 7 are generally discontinuous.

The destructive evaluations corroborated the data gathered from the c-scan images. The c-scan images only showed damage in interfaces 3, 5, 6, and 7 and that the major axis of delamination is along the direction of the back surface ply. The destructive evaluations showed small amounts of delamination in interfaces 1 and 2 but these were generally insignificant and the major axis did always line up with the back surface ply. The destructive evaluations also generally agreed with the c-scans about the size of the delaminations. However, the destructive evaluation data indicates that the assumption that delaminations are always continuous through the dent center may not be correct and in fact, it seems that many of the shielded delaminations from the c-scan are likely discontinuous through the shielded region. So, if we were to simply rely on the c-scan images

without any destructive evaluations to supplement them, it is likely that we would have not come to accurate conclusions about the total amount of delamination. The destructive evaluations also showed no evidence of any debonding within any of the specimens.

C. Effect of Specimen Size

When conducting impact tests on specimens such as these, cost is a major concern. Since a large portion of the costs of this study are material costs, the larger the indented specimen, the greater the cost. So, the specimens used for the destructive evaluation were designed to be as small as possible, without changing the results, i.e. the damage observed within the small specimens should be equivalent to the damage observed within the large specimens. However, in order apply the trends extracted from the destructive evaluations of the small specimens to the large specimens; we must first confirm that indeed, the damage induced within the small specimens is equivalent to that induced within the large specimens.

As stated in the panel manufacturing section, for each indentor size, there were two panel sizes. For specimens indented under the 25.4mm diameter indentor, panels were either 177.8 mm x 152.4 mm or 75 mm square. The convention for these graphs is that the difference in specimen size is shown by different colors. All specimens presented were indented under approximately 1310 N. Comparisons will be made across three panel geometries: Q1-C2, Q2-C1, and Q3-C1 because these are the only geometries with sufficient data on specimens indented under the proper load for comparison.

Figure 14 presents the dent diameter for the various panel geometries and Fig. 15 presents the dent depth for the different material geometries. The only panel geometry with a significant number of data points is Q1-C2. From here, we can get a general feel for the amount of scatter within the data. In both graphs, all three panel geometries appear to be within the scatter established from Q1-C2 for both large and small specimens. Thus, from the data available, it appears that there are no effects of specimen size over the given range of specimen sizes for dent formation.

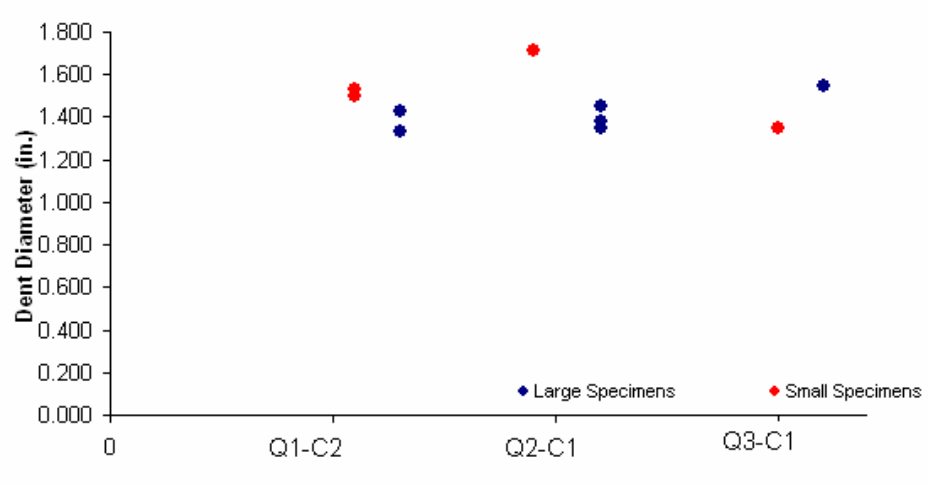

Figure 14. Dent Diameter For Different Panel Geometries

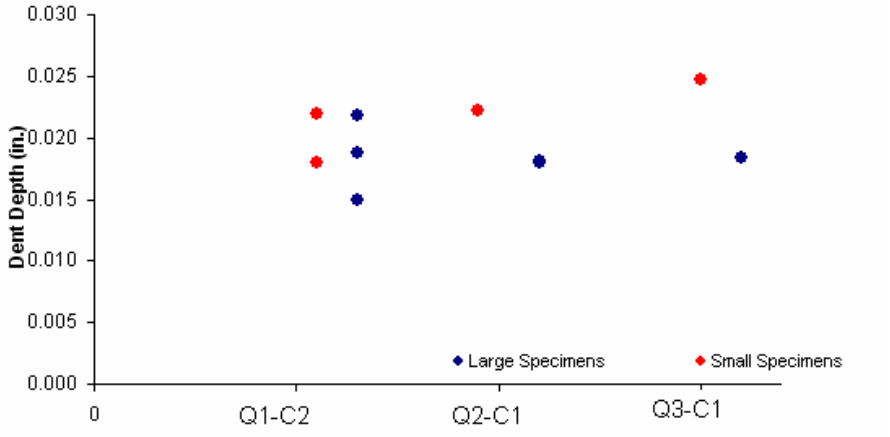

Figure 15. Dent Depth For Different Panel Geometries

Figure 16 presents the planar area of delamination for the different panel geometries. Geometries Q2-C1 and Q3-C1 exhibit similar data for both the large and small specimens. However, the Q1-C2 geometry seems to indicate that the larger specimens contain significantly more delamination than the smaller ones. This discrepancy is probably the result of the quality of the c-scans images more than the actual differences within the specimen. In order to determine the planar area of delamination, only the c-scan images can provide data for the planar area of delamination.

The c-scan images for the small Q1-C2 specimens were among the first to be c-scanned and then the first to be cross-sectioned. Unfortunately, the c-scan technique had not been perfected yet and the quality of the image is very poor as can be seen in Fig. 17. Those specimens could not be rescanned because they had already been cross sectioned. However, a small Q1-C2 specimen with a high quality c-scan image does exist. It was indented well above BVID so it is not included in the graphs, but a qualitative comparison of its c-scan to other Q1-C2 c-scans can be made. Figure 18 presents the c-scan image of this small specimen indented beyond BVID and a large specimen indented at BVID. From a qualitative comparison, the general features such as shape and location of delaminations appear similar.

So, from the available data, it appears that all three of these panel types exhibit no size effects for dent formation and at least Q2-C1 and Q3-C1 exhibit no size effects for delamination damage. It is somewhat ambiguous as to whether there

are size effects in Q1-C2 for delamination damage but there is some evidence to suggest that there is not.

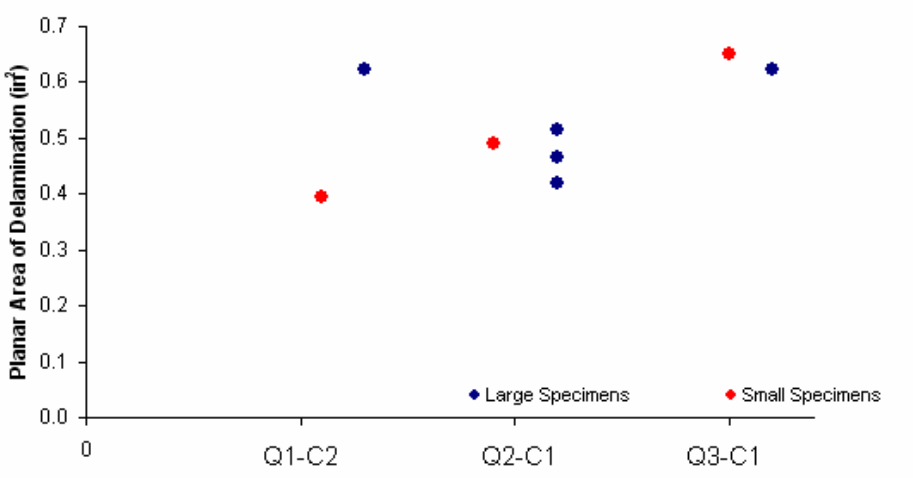

Figure 16. Planar Area of Delamination For Different Panel Geometries

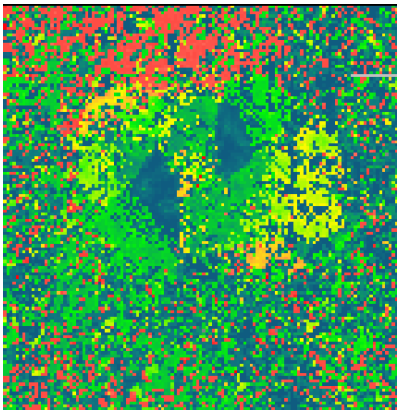

Figure 17. C-scan Image for Q1-C2 Specimen Indented To BVID
The quality of the image is very poor and it is difficult to tell where most of the delaminations begin and end. This is likely a major cause of the discrepancy shown for Q1-C2 in the previous figure.

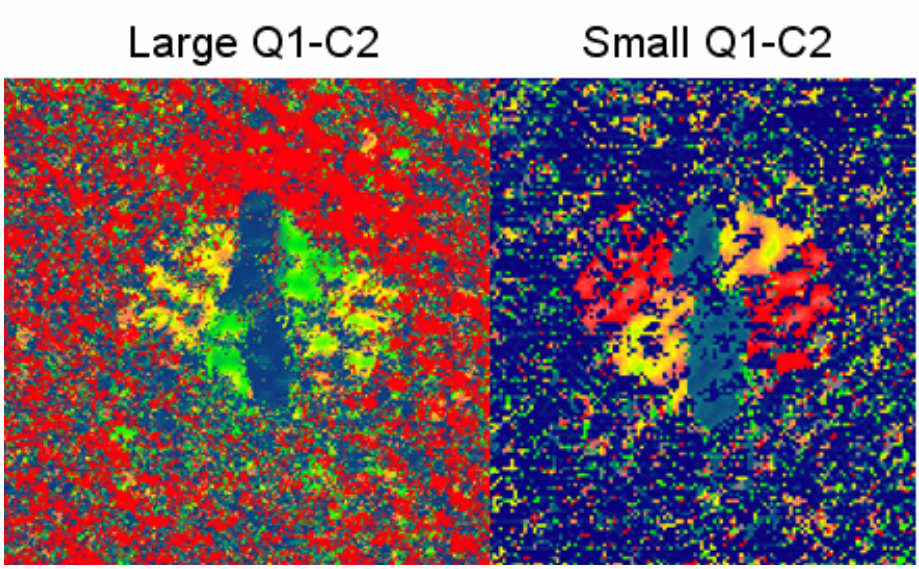

Figure 18. Comparison of Small and Large Q1-C2 Specimens
The small specimen was indented to a load well above BVID but a qualitative comparison between the two. The scale of the images is somewhat different so one cannot rely exclusively on the colors. However, the three delaminations visible appear to be similar in size, shape, and orientation.

D. Damage Resistance

In this section, the methods described above are used to evaluate the damage resistance of the various panel geometries. The definition of "damage resistance" depends on how one defines the damage event. The damage event may be thought of as a particular QSI force and indentor, in which case the damage metrics considered are dent depth, dent diameter and delamination. Alternatively, the damage event could be thought of as imparting a dent of a given depth, in which case only dent diameter and delamination would be metrics of any interest.

In order to be consistent, the graphs presented below only show data for the full size specimens. The full size specimens were chosen because there were more of them so that a larger sample size could be used. Figure 19 presents the average QSI force versus average dent depth for the panels tested under the 25.4mm

diameter indentor. The panels indented under the 12.7mm diameter indentor are left out because there are not enough of them to draw any specific conclusions about parametric effects. As indicated in the legend, different shaped symbols are used to represent the different face sheet types, and different colors are used to represent the different cores. Filled symbols depict specimens that were loaded to the BVID force level, while open symbols depict specimens that were loaded to a higher force. Generally, specimens were loaded to a higher force in order to get the dent depth to match up with that of other specimens. To obtain the average QSI values in the figures, specimens of the same type were first grouped. These were then subdivided into groups that were indented under the same force within 1-2 N. The average force and dent depth were then determined for each group. These average results are presented in order to illustrate general trends. Analogous results for average QSI force versus average dent diameter are presented in Fig. 20.

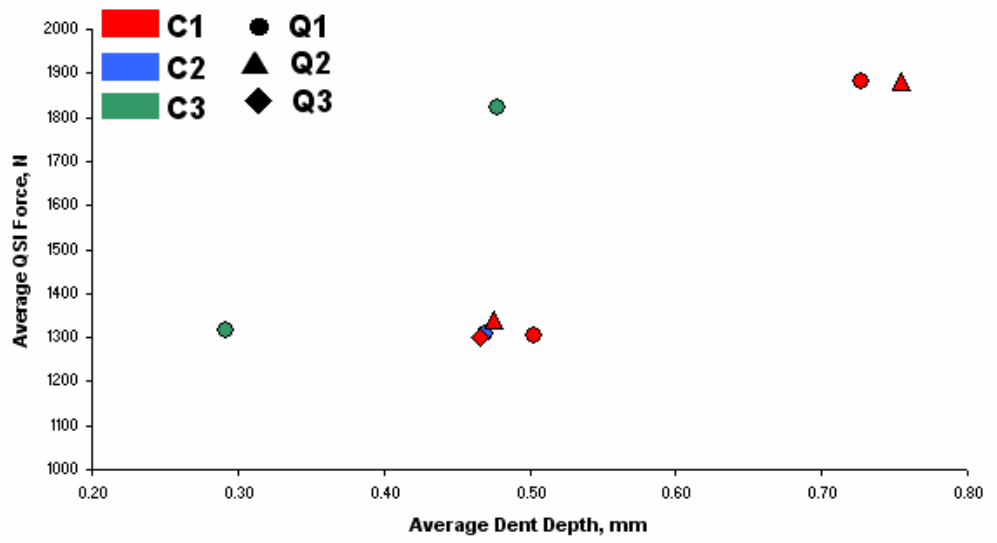

Figure 19. Average QSI Force vs. Average Dent Depth

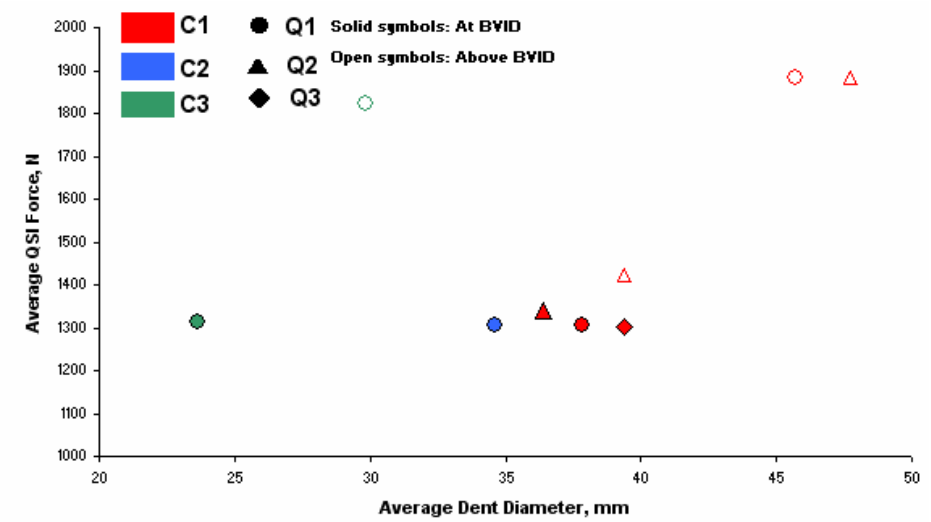

Figure 20. Average QSI Force vs. Average Dent Diameter

When looking at the affect of a particular parameter, all of the other parameters must be held constant. When comparing the effects of core, specimens with the Q1 layup are considered. Conversely, when comparing the effects of layup, specimens with the C1 core are considered. Considering the specimens with the Q1 layup, Figs. 19 and 20 show that, for a given QSI load and indentor, the largest dent depths and areas are observed in those that have the C1 core, the next largest in C2 core specimens, and the smallest dents in C3. Considering specimens with the C1 core, at the BVID force level, specimens with the Q1 face sheet show larger dent depths and diameters than those with Q2. Interestingly, this trend is reversed for the higher force level specimens. Thus if dent depth or dent diameter were the damage metric, the average results show that the C3 core provides the most damage resistant panels and C1 the least, and that the Q2 face sheet is more damage resistant than Q1. Consistent results were not obtained for Q3, and no conclusions can be drawn about this layup.

Figure 21 shows the ratio of dent diameter to dent depth for the various panel types. Interestingly, note that when the force levels are increased so that the dent depth in the C3 core specimens agrees with those in the other specimen types, the dent diameter for C3 remains smaller. The ratio of dent diameter to dent depth is essentially independent of the load level. Specimens with the C3 core clearly show a lower diameter for a given depth. However, although the C2 core was shown to be stiffer than C1, the ratio in Fig. 21 for specimens from the two cores and with the same face sheet is essentially the same. This shows that the ratio of dent diameter to dent depth is a function of core density, and that denser cores will show smaller dent diameters for a given depth.

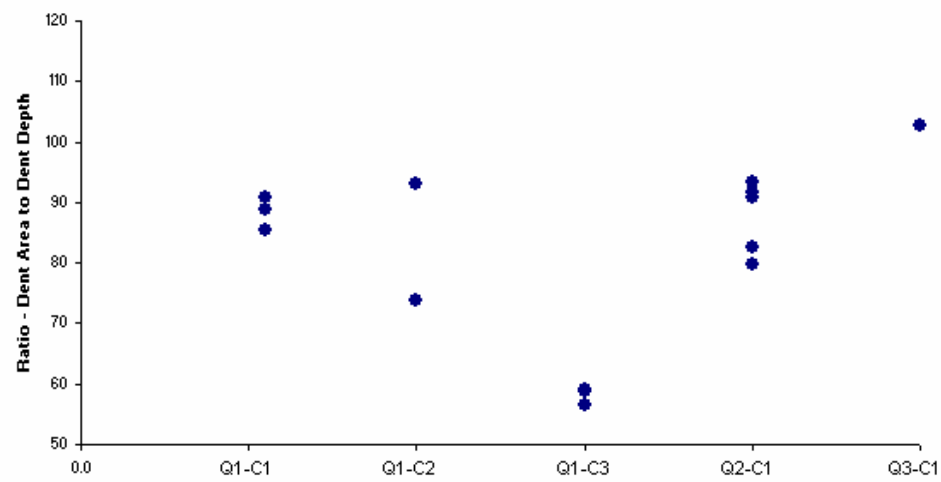

Figure 21. Ratio of Dent Area to Dent Depth

Figure 22 considers the case where planar delamination area is chosen as the damage metric and the damage event is the QSI force. Here, planar delamination area refers to the overall area of delamination that is obtained from the NDE images; the area of potentially shielded delaminations is not included. That is, if one delamination lies on top of another, they are not both counted. To compute

this value, the major and minor axes of the boundary of all delaminations obtained by NDE were first determined. The average of these two values was then defined as the equivalent circular diameter, and the area of this equivalent circle was computed. In order to determine the effect of the face sheet, we first consider specimens with the same core. Considering specimens with the C1 core, if damage resistance is based on QSI force versus planar delaminated area, then specimens with the Q1 face sheet are the most resistant to damage while Q2 is second most with Q3 being the most susceptible to damage. This is most likely related to the fact that Q1 has 45° angle changes between adjacent plies. This results in a lower thermal and mechanical mismatch and therefore lower interlaminar shear stresses during QSI, than what occurs in Q2 and Q3, which have 90° angle changes between adjacent plies. Similar results were reported in Ref. 2.

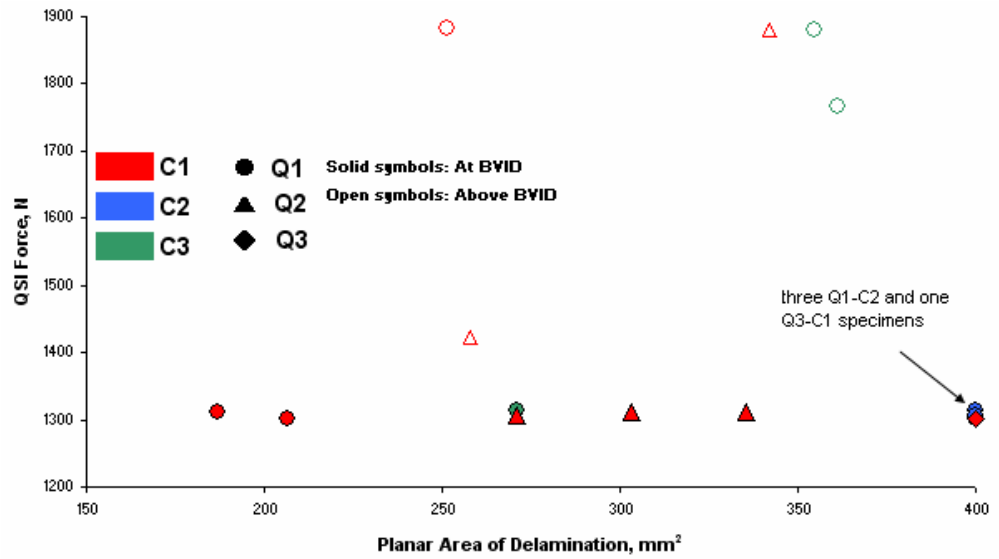

Figure 22. Planar Area of Delamination versus QSI Force

The effect of core on the delaminated area may be observed by comparing specimens with the same face sheet. Specimens with the C1 core show lesser amounts of delamination than those with the C2 or C3 cores. Since the damage due to low velocity impact and QSI has been shown to be essentially the same, it may be easiest to think of this from an energy perspective. Since the C2 and C3 cores are stiffer than C1, less energy is dissipated early on through core crushing. However, this energy must dissipate somehow, and so more energy dissipates via delamination when. There is no clear trend between C2 and C3 so no conclusions can be drawn about them at this time.

Overall, if delamination area is the damage metric, then the Q1 face sheet along with the C1 core will provide the most resistant result. This is in contrast to the case where dent depth or dent area was the metric, where the Q2 face sheet combined with the C3 core provided the best damage resistance, and Q1-C1 was the worst. This is better illustrated in Fig. 23, which shows the ratio of the planar area of delamination to the dent area as a function of panel type. Since dent area and dent depth were shown to follow the same general trend, conclusions from this figure can also be extended to delaminated area versus dent depth. Here, Q1-C1 is observed to have a small amount of delamination for a given dent area, i.e., it shows a large dent area, but a small amount of delamination. Q1-C3 shows the reverse: a small dent area, but a large amount of delamination. Presenting the data in the format of Fig. 23 also appears to indicate that, for a given face sheet, the C2 core type provides intermediate results to the C1 and C3 cores.

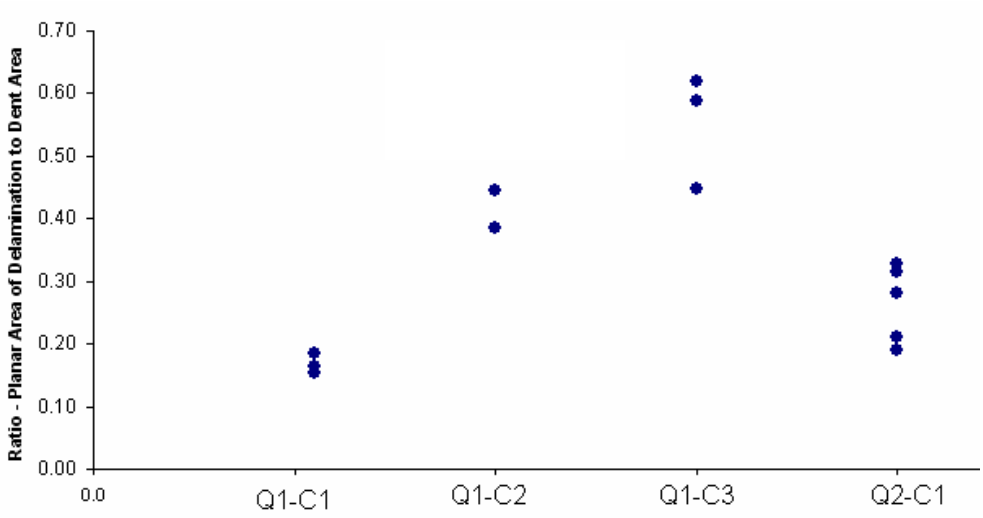

Figure 23. Ratio of Planar Area of Delamination to Dent Area

V. Conclusion

This work considered the effects of core density, core thickness, face sheet layup and indentor diameter on the type and extent of quasi-static indentation damage in aluminum honeycomb core sandwich laminates with eight ply carbon fiber reinforced quasi-isotropic face sheets. The ratio of dent diameter to dent depth was found to depend on core density, where specimens with denser cores show smaller dent diameters for a given depth. That is, outside of the contact region, stiffer cores do a better job resisting crushing by the face sheet.

Regardless of specimen layup, delaminations were observed to occur essentially only at the 3rd, 5th, 6th and 7th interfaces. Delaminations were oblong, with their major axis direction dictated by the angle of the fibers in their back surface ply. One important finding is that deeper delaminations were not always continuous through the dent center, but rather could be split into two distinct areas on either side of it. Stiffer cores, either in terms of a higher density or, for those

cores considered, a smaller thickness, meant more delamination would occur in the face sheets. Regardless of the core, larger delaminations were observed in face sheets that contained only 90° angle changes between adjacent plies in comparison to those that contained only 45° angle changes.

In order to assess the damage resistance of the various specimen types, the damage metrics of dent depth, dent area and planar delaminated area were evaluated. If dent depth or dent diameter is chosen as the damage metric, then more damage resistance is obtained with increasing core density, and a $[\pm 45/0/90]_s$ face sheet was found to be best choice of the three face sheets considered. Lower density cores resulted in a larger permanent dent for a given indentation event, and a low density core with a $[45/90/-45/0]_s$ face sheet was found to be the least damage resistant configuration of those evaluated. On the other hand, if delamination area is the damage metric, then the low density core and the $[45/90/-45/0]_s$ face sheet will provide the *best* damage resistance, i.e., the least amount of delamination for a given indentation event. When considering compression-after-impact response, a deep dent can lead to a global instability or kink band type of failure, whereas a large delamination can lead to failure controlled by delamination buckling and fiber failures.[9] This observation, along with the dramatically different results that were observed for the damage modes among the different specimen types considered in this study, indicates the need for a closely coupled approach to damage resistance and damage tolerance, where the effects of the damage induced in different panel types by the same event can

be predicted under the service loadings of interest. This knowledge may then be used as guidance in the choice of the structural geometry.

VI. Sources cited and consulted

[1] Zakas J. A., T. Nicholas, H. F. Swift, L. B. Greszczuk and D. R. Curran. 1982. *Impact Dynamics*. New York: John Wiley and Sons.

[2] Kim, C.G. and Jun, E., "Impact Resistance of Composite Laminated Sandwich Plates," *Journal of Composite Materials,* Vol. 26, 1992, pp. 2247–2261.

[3]Williamson, J.E. and Lagace, P.A., "Response Mechanisms in the Impact of Graphite/Epoxy Honeycomb Sandwich Panels," *Proceedings of the American Society for Composites Eighth Technical Conference on Composite Materials*, Cleveland, OH, 1993, pp. 287-297.

[4]Herup, E.J. and Palazotto, A.N., "Low-Velocity Impact Damage Initiation in Graphite/Epoxy/Nomex Honeycomb-Sandwich Plates," *Composites Science and Technology*, Vol. 57, 1997, pp. 1581-1598.

[5]Ferri, R. and Sankar, B.V., "A Comparative Study on the Impact Resistance of Composite Laminates and Sandwich Panels," *Thermoplastic Composite Materials*, Vol. 10, 1997, pp. 304-315.

[6]Oplinger, D.W. and Slepetz, J.M., "Impact Damage Tolerance of Graphite/Epoxy Panels," *Foreign Object Impact Damage to Composites, ASTM STP 568,* American Society for Testing and Materials, 1975, pp. 30-48.

[7]Canadian Commercial Vehicles Corporation Website, http://www.ccvbc.com/composite_panels.html, Copyright 2009, April 19th 2010

[8]Davidson, B.D., Michaels, J.E., Sundararaman, V. and Michaels, T.E., "Ultrasonic Imaging of Impact Damaged Composite Panels," *Acoustical Imaging*, Volume 19, H. Ermert and H.-P. Harjes, Eds., Plenum Press, 1992, pp. 589-594.

[9]Czabaj, M.W., Zehnder, A.T., Davidson, B.D., Singh, A.K. and Eisenberg, D.P., "Compression After Impact of Sandwich Composite Structures: Experiments and Modeling," *Proceedings of the 51st AIAA/ASME/ASCE/AHS/ASC Structures, Structural Dynamics, and Materials Conference,* Orlando, FL, April 2010.

VII. Appendices

Capstone Summary

The options for materials that engineers have available to them have become more varied over the last century, particularly in terms of composite materials. Composite Materials refer to any material that is composed of multiple, different materials combined on a macroscopic scale. This is different than a material such as an alloy. An alloy is a solution of multiple metals. Here the metals are combined on a microscopic scale and the atoms are distributed as such. Conversely, reinforced concrete is a typical composite, where the reinforcing steel rods are easily distinguishable from the concrete "matrix." Unfortunately, as the materials themselves become more complex, it becomes increasingly difficult to understand how they will function in various situations. It is crucial that the mechanisms by which composites fail and the factors that influence it are more thoroughly understood.

Composites are extremely advantageous in a variety of ways. Firstly, because they can take advantage of a far wider array of materials than traditional engineering materials, they are capable of having a far greater strength to weight ratio than metals or ceramics. Generally, metals react in the same way regardless of the direction of the stress. Materials that exhibit this behavior are called isotropic. Composite materials can be more precisely designed so that they have a lot of strength in specific critical directions while not wasting size and weight to maintain strength in non-critical directions. Materials that act differently depending on direction are known as anisotropic.

Composite materials have a wide array of possible applications; one important application is in NASA's new Ares I rocket. NASA is funding this project because in a device such as a rocket, the strength to weight ratio is extremely important. By being able to use composites with a greater strength to weight ratio than traditional materials NASA can save significant amounts of money on energy costs.

One widely used class of composites is laminated composites. Laminated composites are comprised of multiple plies of fibrous composite materials. One type of laminated composites which is of particular interest is those that use continuous carbon fiber reinforcement. In plies of this type of material, carbon fibers are oriented in a particular direction and held together in an epoxy matrix. Multiple plies of these carbon fiber matrices can be stacked on top of one another creating a composite laminate. Each ply exhibits exceptional strength in the fiber direction but is relatively susceptible to failure in the non-fiber direction. As will be described subsequently, the laminate is also susceptible to failures that occur in-between the individual plies.

The strength of a material can be thought of as its resistance to a particular type of force. In order to produce a material that can handle forces in different directions, plies can be stacked on top of one another, each with fibers in one of several directions. When the plies are stacked in such a way that there are fibers pointing in the 0°, 90°, 45°, and -45° directions and the fiber direction of each ply is symmetric about the midplane of the stack, then the laminate is said to be "quasi-isotropic." This means that it will respond the same way to a force that is

applied in any in-plane direction. It will respond differently to a force in the out-of-plane, or through the thickness direction, and for this reason it is only quasi-isotropic and not isotropic. Laminated composites for space vehicle applications are typically designed for compression and bending loads. A material's resistance to bending stresses is highly dependant on its second moment of area, which is a function of its thickness. By increasing the structure's thickness, one can improve its resistance to bending stresses. The obvious method of increasing the structure's thickness is to add additional plies. However, while increasing thickness and resistance to bending stresses, this also increases weight. Since one of the main benefits of the carbon fiber composite is its low weight, added weight somewhat defeats the purpose of the laminate in the first place. On the other hand, if a low-density material were placed in the middle of the laminate, then this would increases the thickness of the structure, and hence its resistance to bending, without a significant weight increase. This type of approach is referred to as a "sandwich structure" and is illustrated in Fig. 1. The low density material is the core and the high stiffness and strength material comprise the face sheets. When the face sheets are comprised of a laminated composite, this type of arrangement is typically referred to as a sandwich composite. Sandwich composites therefore provide a highly effective approach to improving a laminate's resistance to bending. Here the face sheets bare the majority of the load

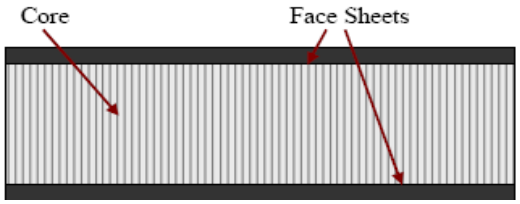

Figure 1. Sandwich Composite
Diagram of typical sandwich composite with face sheets on both ends and the core in the middle

while the core is designed primarily to increase the material's thickness. This effect is similar to that of an I-beam.

Although these sandwich composites possess low weight along with the desired properties of good resistance to bending and compression, they are also susceptible to low velocity impact damage. A low velocity impact could occur in various stages of the material's lifecycle. For instance, during assembly, tools could be dropped upon the specimen or during use, debris or other materials could bump into the panel causing a low velocity impact.

Low velocity impacts result in both external damage, in the form of dents, and internal damage. In general, it is assumed that visibly evident damage (i.e. panels with large dents) will be repaired but damage that is invisible or only barely visible to the naked eye could go unnoticed. Barely visible impact damage (BVID) therefore represents a threshold, such that damage of this size or smaller must be considered to exist in flight structure, and flight vehicle structures must therefore be designed to tolerate this level of damage without a loss in performance. When dealing with metals, one can generally say that if an impact causes little or no external damage, then there is little or no total damage. This cannot be said about sandwich composites. Even if there is little or no visible external damage, there can be enough internal damage to render the panel structurally unsound.

This study investigates the damage induced in sandwich composite specimens if they undergo a low velocity impact, and how various parameters affect that damage. The parameters investigated in this study are the core thickness, core

density, face sheet stacking sequence (the sequence that the plies in various directions are placed on top of one another), load, and indentor diameter. This damage is evaluated through non-destructive means via ultrasonics and destructive means via cross sectioning. The data from these two types of evaluation are compared for consistency and synthesized. A parallel and complementary study is being performed that investigates how much planar compressive strength is lost due to BVID. The results from my study are directly used in this complementary study, as it allows the correlation of various specific damage types to the observed strength loss. Thus, the results of this research are two-fold. First, my study will directly provide knowledge of how different structural and impact parameters affect the internal damage in a sandwich composite. The parallel strength study will provide knowledge about how each type of damage affects the structure's strength. This information may then be used by NASA to choose appropriate structural configurations that will be the most impact resistant.